

SUPPLEMENTARY INFORMATION

**Giant supermagnonic Bloch point velocities in cylindrical ferromagnetic
nanowires**

Felipe Tejo

Universidad Central de Chile, Escuela de Ingeniería, Santiago de Chile, 8330601, Chile.

Jose Angel Fernandez-Roldan

*Institute of Ion Beam Physics and Materials Research, Helmholtz-Zentrum
Dresden-Rossendorf e.V., Bautzner Landstrasse 400, Dresden, 01328, Germany.*

Konstantin Y. Guslienko

*Depto. Polímeros y Materiales Avanzados: Física, Química y Tecnología,
Universidad del País Vasco, UPV/EHU, San Sebastian, 20018, Spain. and
IKERBASQUE, the Basque Foundation for Science, Bilbao, 48009, Spain.*

Rubén M. Otxoa

*Hitachi Cambridge Laboratory, J. J. Thomson
Avenue, Cambridge, CB3 0HE, United Kingdom. and
Donostia International Physics Center, San Sebastian, 20018, Spain.*

Oksana Chubykalo-Fesenko

*Instituto de Ciencia de Materiales de Madrid, CSIC, Cantoblanco,
28049 Madrid, Spain. E-mail: oksana@icmm.csic.es*

I. ADDITIONAL EXAMPLES OF THE BP-DW DYNAMICS.

To study the influence of the nanowire size on the magnetization dynamics, we have additionally calculated the Bloch-point (BP) position and the effective Domain Wall (DW) position when moving through a nanowire of $R = 20$ nm ($L = 1200$ nm) and 40 nm ($L = 2500$ nm). Figure S1 summarizes our results.

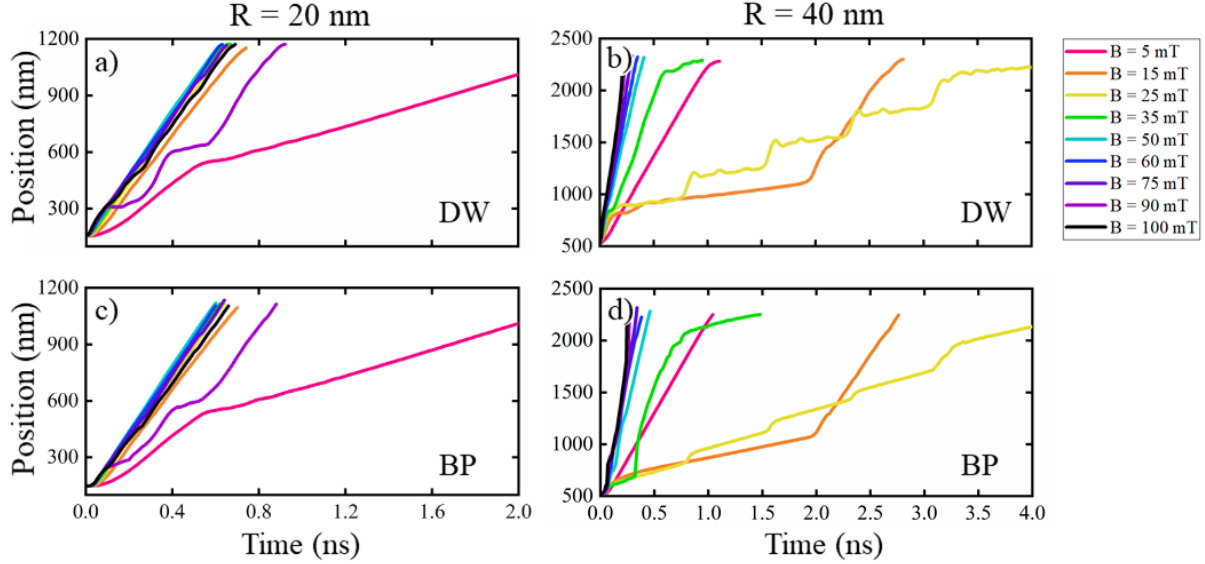


FIG. S1. a), b) Effective DW position evaluated from the dynamics of the longitudinal magnetization component $\langle m_x \rangle(t)$, as its zero crossing point as a function of time for $R = 20$ nm and $R = 40$ nm, respectively. c), d) Bloch-point position as a function of time for $R = 20$ nm and $R = 40$ nm, respectively.

Furthermore, we have calculated the maximum velocity of the BP when it is driven, by an external magnetic field, through a nanowire with three different radii. As in the main text, we have considered a cell size of $1 \times 1 \times 1 \text{ nm}^3$ and a damping of $\alpha = 0.01$. Figure S2 shows our results for radii $R = 20$, $R = 30$, and $R = 40 \text{ nm}$.

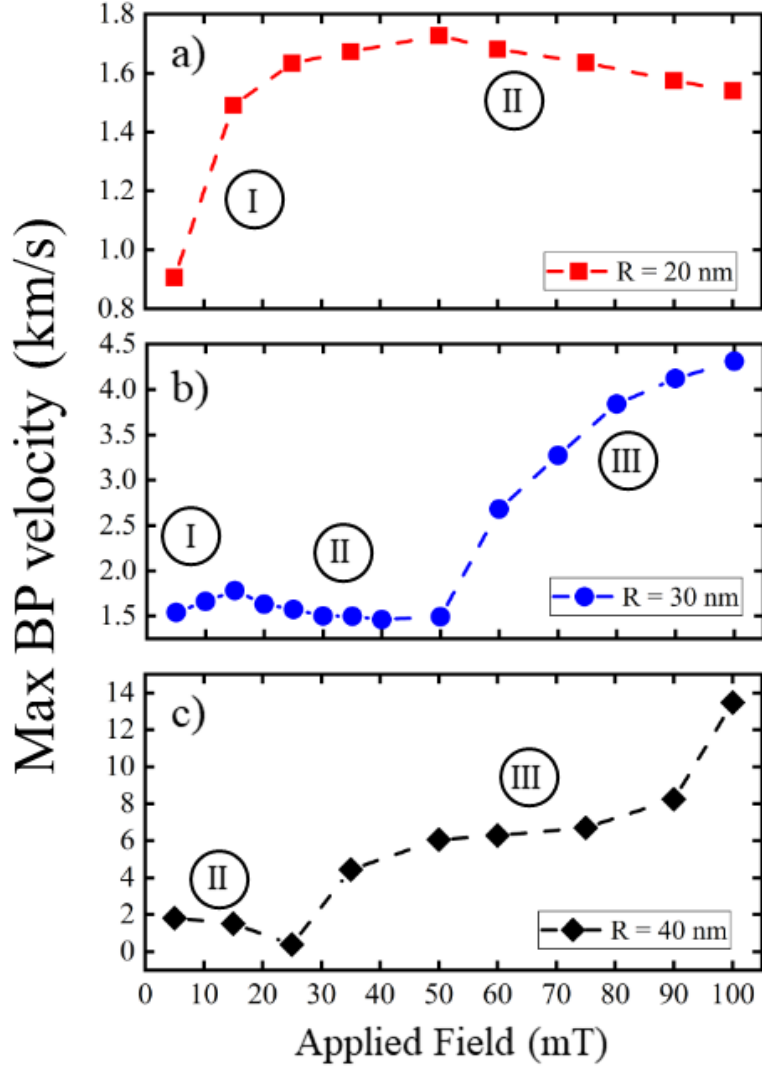


FIG. S2. Comparison of the maximum BP velocities as a function of the applied magnetic field for three different radii: $R=20$, $R=30$, and $R = 40 \text{ nm}$.

To better understand the magnetization dynamics, we represent the DW structure (internal and external, i.e., on the surface) at different time instants. For this purpose, we have considered an applied magnetic fields of magnitude $B = 15$, $B = 35$, and $B = 100$ mT. The results are presented in Figs. S3, S4, S5, respectively. The case of $B = 15$ mT (Fig.S3) corresponds to regime II and illustrates the spin-Cherenkov effect when the DW cone is only slightly elongated and there is a strong backward emission of small-amplitude spin waves. The case $B = 35$ mT (Fig.S4) also corresponds to regime II but here a dynamical transformation of the Bloch point domain wall to the vortex-antivortex domain wall and back occurs. Finally, the case $B = 100$ mT (Fig.S5) corresponds to regime III where DW elongates and breaks. Large-amplitude spinwaves are visible on the nanowire surface.

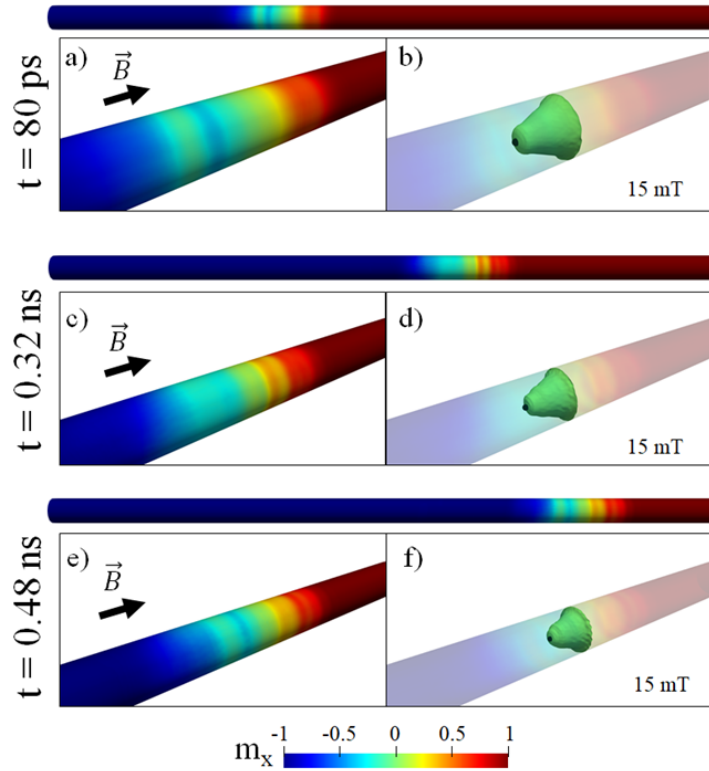


FIG. S3. Snapshots of the magnetization dynamics when a magnetic field of 15 mT is applied. a), c) and e) show the surface magnetization of the DW at different times, while b), d) and f) show their corresponding internal structures.

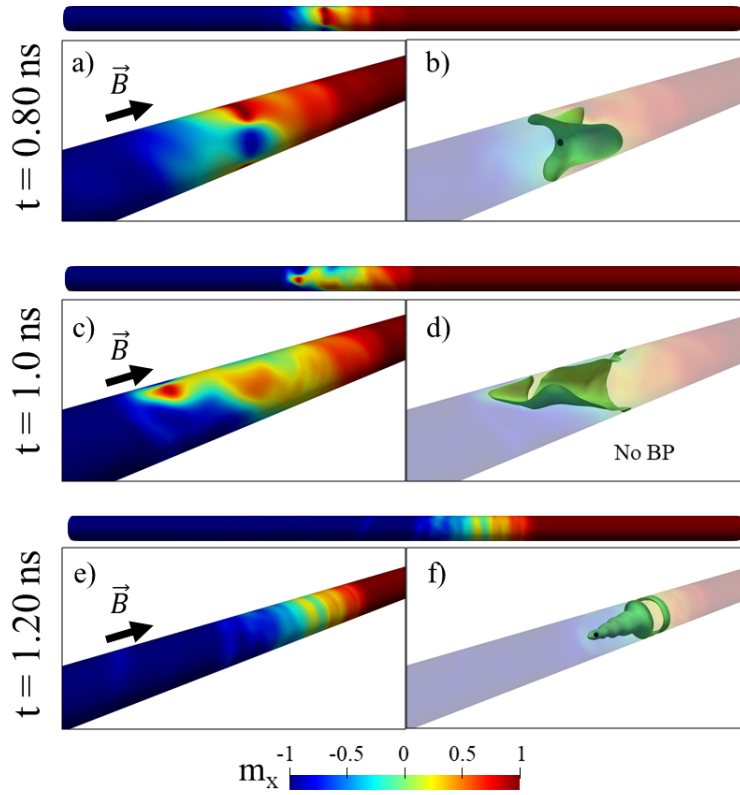


FIG. S4. Snapshots of the magnetization dynamics when a magnetic field of 35 mT is applied. a), c) and e) show the surface magnetization of the DW at different times, while b), d) and f) show their corresponding internal structures. It is possible to notice that in d), the BP disappears due to complex magnetization dynamics.

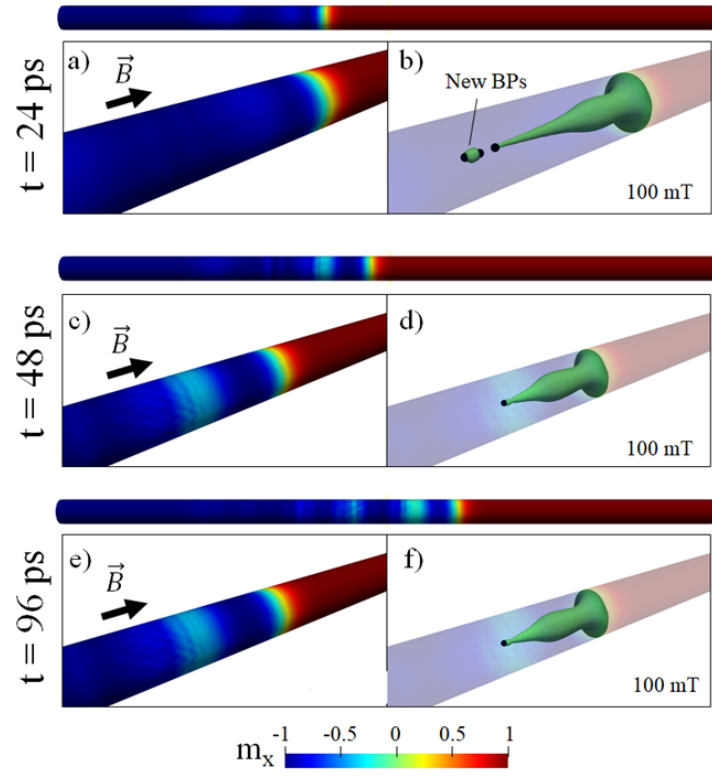


FIG. S5. Snapshots of the magnetization dynamics when a magnetic field of 100 mT is applied. a), c) and e) show the surface magnetization of the DW at different times, while b), d) and f) show their corresponding internal structures.

As it was mentioned, on the surface of the nanowire spinwaves of cylindrical symmetry are clearly visible. In the turbulent regime III, these spinwaves are of large amplitude. We have estimated the spin-wave group velocity using micromagnetic simulations, for nanowire of 30 nm diameter (as in the main text), see Fig.S6. For this purpose, we have studied the propagation velocity of the wavefront when the spin wave reaches two different points on the nanowire surface 30 nanometers from each other. Note that in the region highlighted by a blue square magnetisation component m_y reaches the value close to -1, meaning that the base of the DW cone reached these point at ca.0.15 ns. Spinwave maximum reaches these points at ca. 0.22 ns. At this moment new Bloch points are born and the Bloch point, attached to the main cone is situated approximately at $0.98 \mu\text{m}$ from the left nanowire end, i.e. slightly in front. From the time delay of surface spinwaves at two points (red and black curves), we evaluate the spinwave velocity $v_{sw} = 3333 \text{ m/s}$, exactly the same as the Bloch point one. Thus the spinwave maximum is related to the annihilation of the new Bloch points.

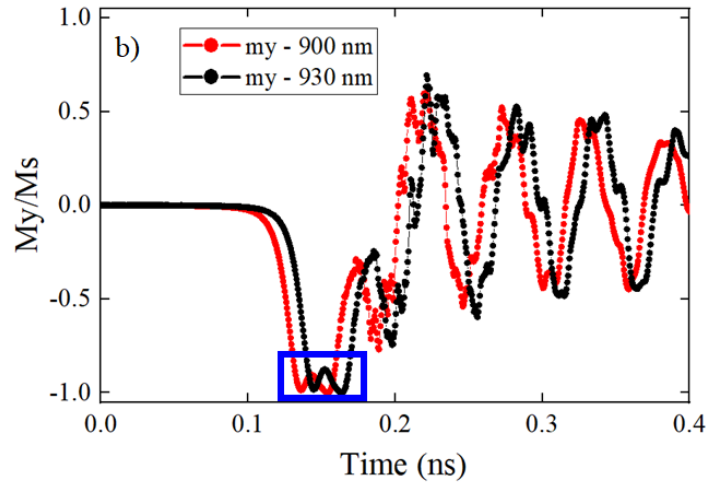


FIG. S6. The motion of a non-rigid BP-DW (due to a magnetic field of 70 mT through a nanowire of 1500 nm length and 30 nm radius) produces spinwaves on the nanowire surface. The wavefront of the emitted spin waves reaches two points situated at 900 and 930 nm from the nanowire end on the surface (red and black curves) with a time delay of $\Delta t = 0.0136 \text{ ns}$. The square highlights points when the base of the domain wall cone reached the points

Fig. S7 shows the amount of Bloch points generated during the domain wall dynamics in a nanowire with a 30 nm radius under 100 mT applied field.

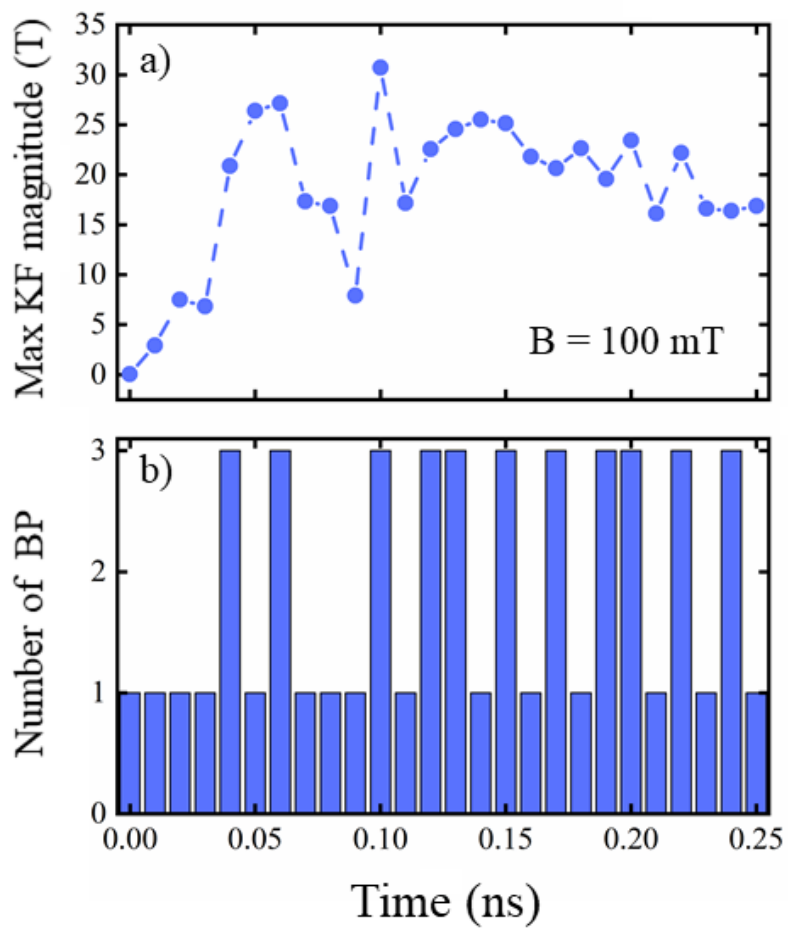


FIG. S7. a) Maximum magnitude of the kinetic field and b) Amount of BPs in the nanowire as a function of time when a magnetic field of 100 mT is applied.

Next, Fig. S8 presents enlarged images during the birth of new Bloch points, illustrating their polarities and chiralities.

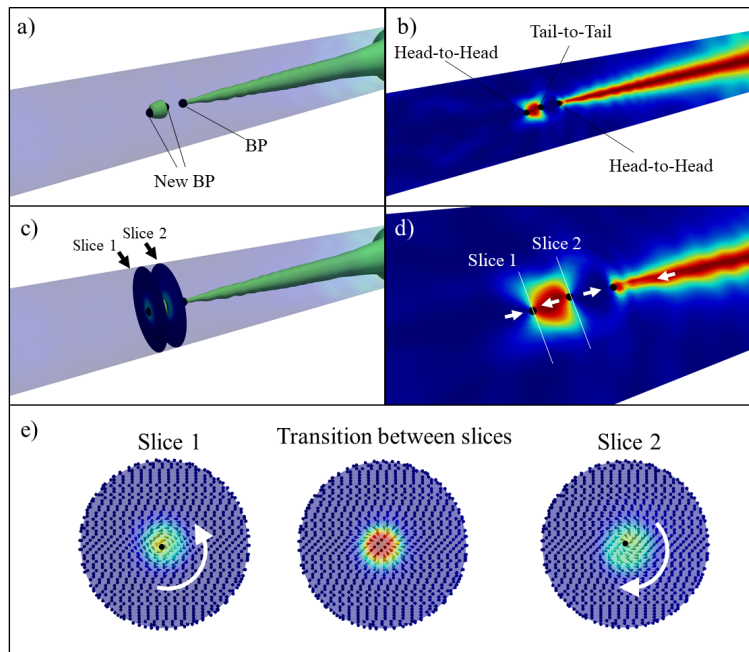


FIG. S8. Snapshots of the magnetization dynamics when a magnetic field of 60 mT is applied. a) show the domain wall magnetization internal configurations at $t = 0.36$ ns. b) shows the magnetization in a cross-section along the wire, identifying the BP configuration (Tail-to-Tail or Head-to-Head). d) is a zoom of b). The white arrows indicate the direction of magnetization. c) shows two cross-sections at the position of the new BP, whose magnetization configuration shows in detail in e).

It is well known that The Bloch point is a singularity in the continuous approximation and therefore, a dependence on the discretization size can be expected. In order to study the influence of the system discretization size, we have calculated the maximum BP velocity using three different computational cell sizes. Figure S9 summarizes our results for a 30 nm radius nanowire.

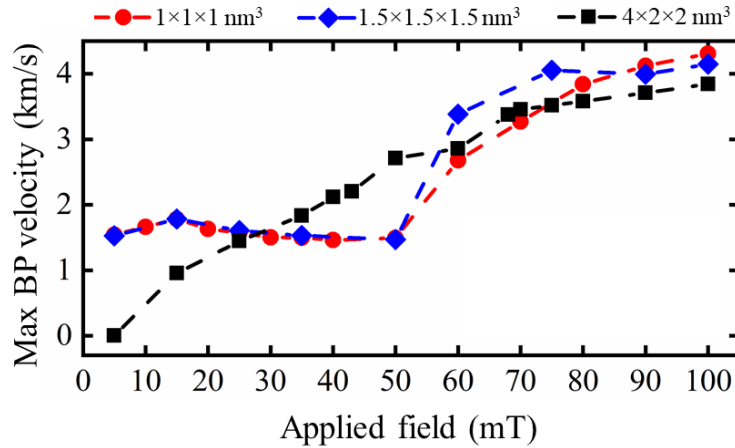


FIG. S9. Maximum BP velocity as a function of applied magnetic field for three different cell sizes.

Finally, we would like to point out that the system behavior under the action of high magnetic fields is not trivial. We have seen that at high fields the system enters the “turbulent” behavior. We present below a limiting case for a magnetic field of 500 mT. Figure S10 presents two snapshots of the magnetization configuration, revealing a marked distortion in the domain wall between the two-time moments (0.03 and 0.12 ns), suggesting the occurrence of complex transformations. At 0.12 ns the domain wall is broken in several places.

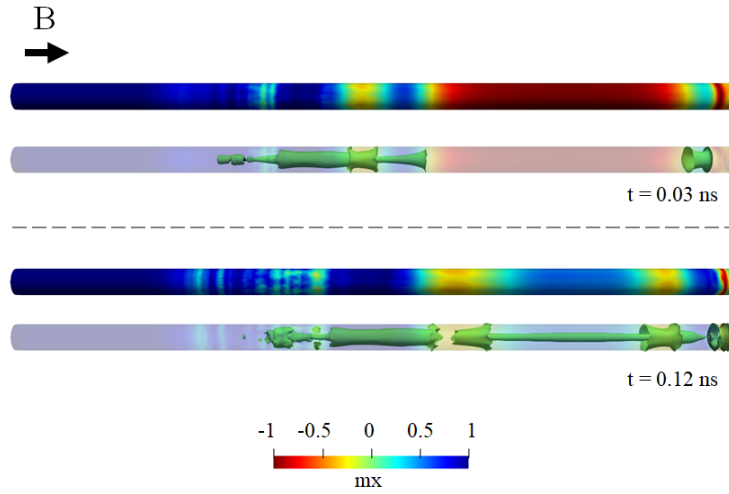


FIG. S10. Snapshots of the magnetization dynamics when a magnetic field of 500 mT is applied for to the nanowire with $R = 30 \text{ nm}$ and cell size $1 \times 1 \times 1 \text{ nm}^3$. The upper panels show the surface magnetisation while the lower ones illustrate the internal magnetic structure. This limiting case demonstrates that for high fields, the dynamics of the system become very complicated. .

II. THEORETICAL ESTIMATION OF THE SPIN WAVE VELOCITIES

Let us consider a cylindrical nanowire of radius R and length L made of soft magnetic material. We assume that for given nanowire sizes and magnetic parameters, the nanowire is in a single-domain state with homogeneous magnetization \mathbf{M}_0 directed along the wire length (coordinate z). The goal is to calculate the spin wave dispersion relations and phase spin wave (SW) velocities for the lowest modes propagating along the wire length. This is a complicated problem due to the existence of the non-local magnetostatic interaction. The problem was considered numerically in the previous papers [1, 2]. To get an analytical description of the problem, we use the Herring-Kittel SW dispersion relation derived for infinite ferromagnetic media and account for a finite wire radius R in the XY plane. The magnetization is $\mathbf{M}(\mathbf{r}, t) = \mathbf{M}_0 + \mathbf{m}(\mathbf{r}, t)$. The radius vector in the cylindrical coordinates $\mathbf{r} = (\rho, \varphi, z)$. The boundary condition for dynamical magnetization \mathbf{m} is at the nanowire circumference $\rho = R$ is $\partial \mathbf{m} / \partial \rho = 0$.

The dynamical magnetization $\mathbf{m}(\rho, \varphi, z, t)$ can be represented as a linear combination of the eigenfunctions numbered by indices n and m , $J_m(\kappa_n \rho) \exp[i(m\varphi + kz - \omega t)]$, where $J_m(x)$ is the Bessel function of the first kind, κ_n is the quantized radial component of the wave vector, and the wave vector k along the wire length is continuous. We are interested in the azimuthally symmetric modes, $m = 0$. Therefore, the values of κ_n are $\kappa_n = \alpha_n/R$, where α_n are determined from the equation $J_1(\alpha_n) = 0$, $n = 1, 2, \dots$

The Herring-Kittel dispersion relation for the cylindrical geometry is:

$$\frac{\omega_n(k, \alpha_n)}{\omega_M} = \sqrt{\left[h + \left(\frac{l_e}{R} \right)^2 (k^2 + \alpha_n^2) \right] \left[h + \left(\frac{l_e}{R} \right)^2 (k^2 + \alpha_n^2) + \frac{\alpha_n^2}{k^2 + \alpha_n^2} \right]}, \quad (1)$$

where $\omega_M = \gamma 4\pi M_s$, $h = H_z/4\pi M_s$ is the reduced magnetic field along the nanowire length, $l_e = \sqrt{A/2\pi M_s^2}$, is the material exchange length, and wave vector k is in units of $1/R$.

We use the parameters of Fe: the exchange stiffness $A = 21$ pJ/m, the saturation magnetization $M_s = 1700$ kA/m, and the gyromagnetic ratio $\gamma/2\pi = 29.0$ GHz/T. This yields the exchange length $l_e = 3.40$ nm and $\omega_M/2\pi = 61.9$ GHz. The nanowire radius varies within the range $R = 30 - 50$ nm. The typical SW dispersion relation is shown below in Fig. SS11 for $R = 30$ nm and, $h = 0.01$ (normalized to $4\pi M_s$, i.e. 21.4 mT).

The SW frequencies monotonically increase with the wave vector k increasing because of the relatively small value of R . The SW phase velocity is $v(k, \alpha_n) = \omega_n(k, \alpha_n)/k$, see Fig. SS12. The

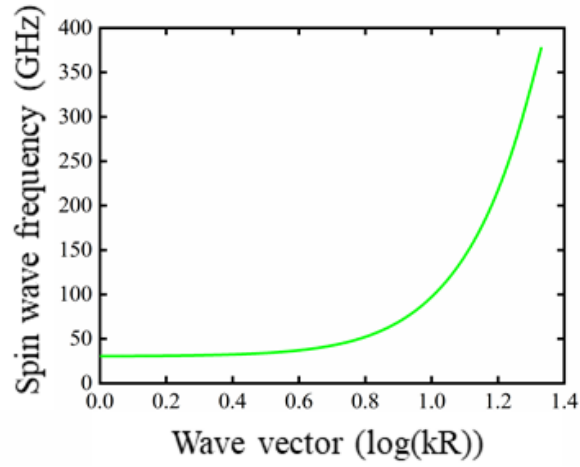


FIG. S11. The SW dispersion relations for the azimuthal symmetric modes are calculated by Eq. (1). $R = 30$ nm, $h = 0.01$.

minimal SW phase velocity for the given SW mode is a function of the nanowire radius, R , and bias magnetic field, h , see Fig. SS13. The typical values of $v_{min}(k, \alpha_n)$ are 1.5 – 1.8 km/s for the Fe nanowires.

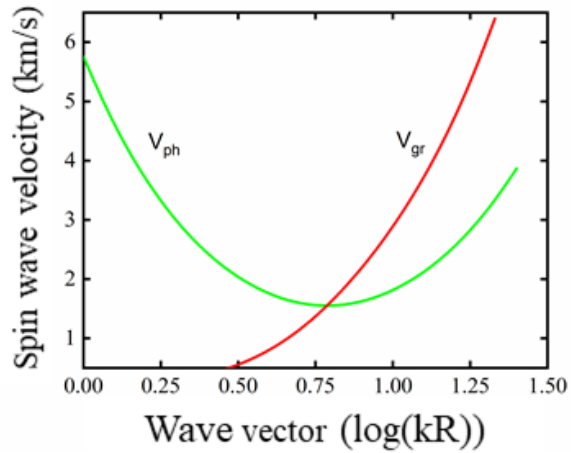


FIG. S12. SW phase velocity of the lowest SW mode ($n=1$) for the nanowire radius $R = 30$ nm and $h = 0.01$.

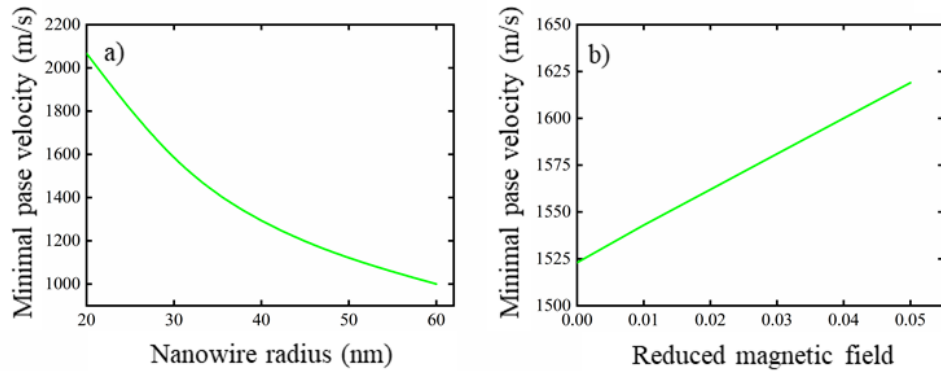


FIG. S13. The dependence of the minimal SW phase velocity on the dot radius and on the bias magnetic field along the nanowire axis ($R = 30$ nm).

-
- [1] R. Arias, , and D.L. Mills. Theory of spin excitations and the microwave response of cylindrical ferromagnetic nanowires. Phys.Rev.B, 63:134439, 2001.
- [2] J. Rychly, V.S. Tkachenko, J. W. Klos, A. Kuchko, and M. Krawczyk. Spin wave modes in a cylindrical nanowire in crossover dipolar-exchange regime. J. Phys. D., 52:075003, 2019.